

Finite Element Method Using PDETOOL of Matlab for Hybrid Stepper Motor Design

E.V.C. Sekhara Rao^{*1}, P.V.N. Prasad²

¹Chaitanya Bharathi Institute of Technology (CBIT), Hyderabad, India

²University College of Engineering (UCE), Hyderabad, India

e-mail: chandrasekharev@yahoo.co.in*, polaki@rediffmail.com

Abstrak

Makalah ini menyajikan delapan topologi rancangan motor langkah magnet permanent hibrida khususnya tentang analisis unjuk kerja rangkaian magnetik berdasarkan metode elemen hingga yang terdapat dalam PDETOOL dari perangkat lunak Matlab. Topologi dirancang sesuai jumlah gigi stator dan panjang celah udara. Analisis ini digunakan untuk mengetahui distribusi gaya gerak magnetik (mmf) yang disebabkan oleh magnet permanen dan kumparan penguatan. Analisis ini akan membantu pemilihan rancangan terbaik berdasarkan distribusi mmf yang lebih baik.

Kata kunci: FEM, PDE toolbox, PMH motor stepper

Abstract

This paper presents eight topologies design of permanent magnet hybrid (PMH) stepper motor for its magnetic circuit performance analysis using finite element method by PDETOOL of Matlab. The topologies are designed according to the number of stator teeth and length of airgap. This analysis is used to know mmf distribution due to permanent magnet and by excitation coil. This analysis helps to chose best design topology for better mmf distribution.

Keywords: FEM, PDE toolbox, PMH stepper motor

1. Introduction

Stepper motor is a special motor used for discrete torque without any interface. Many techniquis like direct torque control (DTC) may raplace applications of induction motor or servomotor with permanent maget synchronous motor (PMSM) [1] but could not replace stepper motor. It is classified into three major types as permanent magnet stepper motor, Variable reluctance stepper motor and Permanent magnet hybrid (PMH) stepper motor [2]. Among all PMH motor is widely used in many applications such as solar array tracking system in satellites, robotics and CNC machines due to its micro-stepping quality with high torque capacities [3]. But its magnetic circuit analysis is complicated due to the presence of permanent magnet and double slotting which is not discussed in detail in [4]. Its magnetic circuit is explained earlier with equivalent circuit model with linear assumsions in [2], [3].

Airgap variation effect on mmf distribution is explained in [4] using equivalent circuit model without considering exact topology of motor. This method is unable to give detail explanation for different topologies mmf distribution.

But getting operating point mmf with permanent magnet is complicated. Finite element model is used for getting accurate operating point of permanent magnet using tooth layer unit [5]. But mmf distribution was not explained in detail for different topologies.

Fem analysis is carried for mmf distribution with different tooth geometries in [6] but variation of materials and current densities are not discussed in detail and analysis is carried using commercial software.

In this paper the FEM analysis of the PMH stepper motor are done using fundamenta concepts of permanent magnet motors [8], [9]. FEM analysis is done using Matlab simulations [7] but PDE toolbox of Matlab is used for design and analysis of PMH stepper motor magnetic circuit first time which is a non-commercial software [10], [11]. PDE toolbox has both command mode and GUI mode. In this paper GUI mode is used to develop the required geometry of the

PMH stepper motor then required boundary conditions are applied then solution is obtained through FEM relations for eight topologies.

Topologies are considered with variation in airgap, stator number of teeth. Two core materials are considered for stator and rotor (Iron (99.8%), Iron (99.95%). Two current densities are considered for analysis (0.5 A, 1 A).

2. Research Method

Tooth layer unit (TLU) [3] is a rectangle area that has a tooth pitch width and two parallel lines behind the teeth of stator and rotor. The area is shown in Figure 1. The factors of the nonlinear material and the non-uniform distribution of magnetic field in the teeth of stator and rotor are taken full consideration in this computation model. There are two basic assumed conditions in the computation model of TLU.

- (i) The lines AB and CD of the TLU in Figure 1 are thought as iso-potential lines.
- (ii) The magnetic edge effect of stator pole is ignored, which is assumed that the distribution of the magnetic field for every tooth pitch width is the same.

Figure 1 shows stator and rotor tooth geometry for one tooth pitch. In Figure 1, u_s , and u_r are scalar quantities of the iso-potential lines AB and CD. The magnetic potential difference F is given by

$$F = U_s - U_r \quad (1)$$

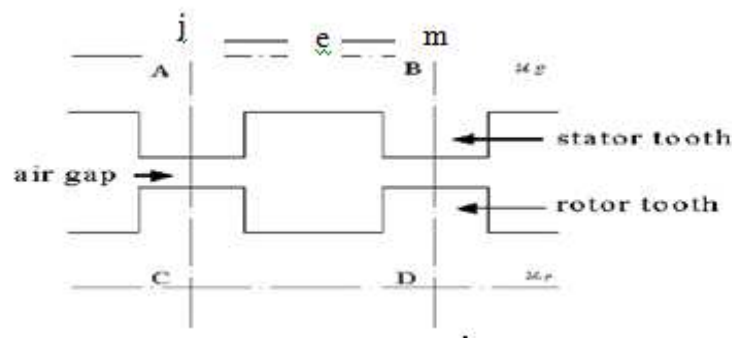


Figure 1. The tooth layer unit

If $\Phi(\alpha)$ is assumed as the flux in a tooth pitch width and per axial unit length of iron core, α is the relative position angle of stator and rotor. The specific magnetic conductance G of TLU is then given by

$$G = \frac{\Phi(\alpha)}{F} \quad (2)$$

Apparently, G is related to the saturation extent of iron core and is changed with F and the relative position angle α . G can be got by the numerical computation on the magnetic field of TLU shown in Figure 1. The lines AC and BD are the periodic boundary lines because the distribution of the magnetic field is considered as the same for every tooth pitch width. The magnetic field in TLU is irrational field and the magnetic equations [2] for the field are given in the rectangular coordinates by

$$\begin{aligned} \frac{\partial}{\partial x} \left(\mu \frac{\partial \varphi}{\partial x} \right) + \frac{\partial}{\partial y} \left(\mu \frac{\partial \varphi}{\partial y} \right) \\ \varphi_{CD} = 0 \\ \varphi_{AB} = 0 \\ \varphi(x, y)_{AC} = \varphi(x + \lambda, y)_{BD} \end{aligned} \quad (3)$$

where φ is the scalar quantity, μ is the magnetic permeability and λ is the tooth pitch. For a certain position angle α and a magnetic potential difference F , the distribution of the magnetic field of TLU can be calculated by the 2D finite element analysis. The flux per axial length of TLU is given in (4).

$$\varphi(\alpha, F) = \sum B_e (\overline{jm})_e \quad (4)$$

Here the nodes j and m are on the border AB as shown in Figure 1. (\overline{jm}) is the length of unit e from node j to m and B_e is the flux density. The specific magnetic conductance G will be used in the calculation of the whole nonlinear network equations of the motor.

Though TLU, the key calculation model of the method is simple in drawing, its calculation model contains some approximate factors due to the basic assumed conditions. It is the main issue to be studied in this paper whether the assumed conditions are of engineering rationality or whether the assumed conditions are in agreement with the practical situations and whether the errors from the assumed conditions can be ignored from the point view of engineering. The two basic assumed conditions (i) and (ii) mentioned are analyzed below. A practical PMH stepper motor was chosen to analyze the rationality. It has 4 poles in the stator and 6 sections in the rotor with disc of NdFeB magnet axially magnetized. The main structure parameters of the motor are shown in Table I.

As the motor is symmetrical, pair of poles of the motor has been chosen as the magnetic numerical calculation area, the magnetic field contains the nonlinear material, iron core, and the current area. The surface arc effect of the iron core and the pole edge effect of the stator are considered in the calculation model, by which the magnetic potential values and their differences on the lines behind the teeth could be found out and the engineering rationality of the assumed conditions could be verified. There is only axial current in Figure 2 and the magnetic potential vector A_z suits Poisson's equation [4], [5] as

$$\left. \begin{aligned} \frac{\partial A_z}{\partial x} &= \frac{b_i A_{zi} + b_j A_{zj} + b_m A_{zm}}{2\Delta} \\ \frac{\partial A_z}{\partial y} &= \frac{c_i A_{zi} + c_j A_{zj} + c_m A_{zm}}{2\Delta} \\ B_x &= \frac{\partial A_z}{\partial y} \\ B_y &= \frac{\partial A_z}{\partial x} \end{aligned} \right\} \quad (5)$$

Δ is the area of the split triangle unit, b_i , b_j , b_m and c_i , c_j , c_m are the parameters of the split triangle unit.

Table 1. Data of PMH stepper motor

Stator poles	Tooth per stator pole	Outside diameter of stator	Inside diameter of stator	Outside diameter of stator shell
04	8	10.108cm	5.936cm	10.652cm
Tooth number of rotor	Number of turns per phase	Section length of rotor	Outside diameter of rotor	Inside diameter of rotor
50	21	10.26cm	4.2cm	1.74cm

3. Results and Analysis

3.1. Geometry Design

Using graphical user interface (GUI) of PDE toolbox of Matlab [6]-[7], geometry of motor is designed for one pole pitch due to symmetry. Rotor is designed with 23 slots with equal spacing and then stator poles are designed with 05 slots for each pole for the above mentioned dimensions. Current coil is designed on stator pole. The obtained geometry is Figure 2 for uniform airgap and Figure 3 for non uniform airgap. Then stator outer shell is designed and the boundary conditions are provided with set formula as

$$(((R_1)+(R_3))(C_3+SQ_1+SQ_2+SQ_3+SQ_7+SQ_8+SQ_9+SQ_{25}+SQ_{26}+SQ_{27}+SQ_{28}+SQ_{29}+SQ_{30}))+((C_2-SQ_4-SQ_5-SQ_6-SQ_{10}-SQ_{11}-SQ_{12}-SQ_{13}-SQ_{14}-SQ_{15}-SQ_{16}-SQ_{17}-SQ_{18}-SQ_{19}-SQ_{21}-SQ_{20}-SQ_{22}-SQ_{23}-SQ_{24}-SQ_{37}-SQ_{38}-SQ_{39}-SQ_{40}-SQ_{41}))+((R_2+R_4)-C_4)+R_5+SQ_{42}+C_6+C_5+C_1)*SQ_{43})$$

where R_1, R_2 are designed for stator pole 1 and R_5 is designed as current coil on pole1. R_4, R_5 are designed for stator pole 2 and SQ_{42} is designed as current coil on pole2. $SQ_1, SQ_2, SQ_3, SQ_7, SQ_8, SQ_9, SQ_{25}, SQ_{26}, SQ_{27}$ are designed as teeth on stator poles. $SQ_4-SQ_5-SQ_6-SQ_{10}-SQ_{11}-SQ_{12}-SQ_{13}-SQ_{14}-SQ_{15}-SQ_{16}-SQ_{17}-SQ_{18}-SQ_{19}-SQ_{21}-SQ_{20}-SQ_{22}-SQ_{23}-SQ_{24}-SQ_{37}-SQ_{38}-SQ_{39}-SQ_{40}-SQ_{41}$ are created equally to provide 23 rotor teeth. SQ_{43} is to provide the required boundary. R_6 is the extra teeth on stator for smooth performance of the motor. From the mentioned set formula (8) the geometry is obtained as shown in Figure 2 for uniform airgap with extra teeth on stator and Figure 3 for uniform airgap without extra teeth on stator.

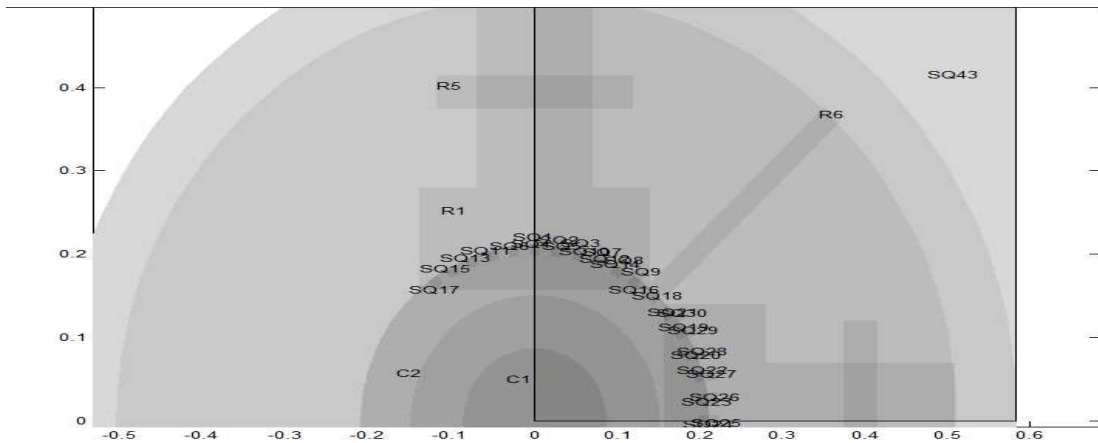


Figure 2. Stator rotor geometry of PMH stepper motor for uniform narrow air-gap (0.137 mm) with extra teeth on stator

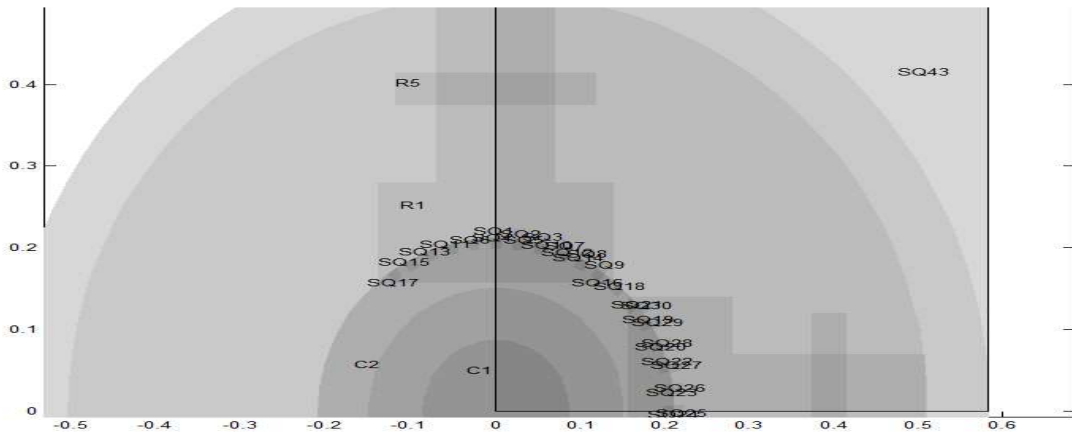


Figure 3. Stator rotor geometry of PMH stepper motor for uniform narrow air-gap (0.137 mm) without extra teeth on stator.

3.2. Motor Boundary Conditions

For getting magnetic potential at the border Dirichlet boundary condition is considered as (1, 0) and Neumann condition specified as (0, 0).

Figure 5 and Figure 6 show geometry for one pole pitch for uniform airgap with and without extra teeth on stator respectively after Dirichlet boundary condition is implied on the design shown in Figure 5, Figure 6 respectively.

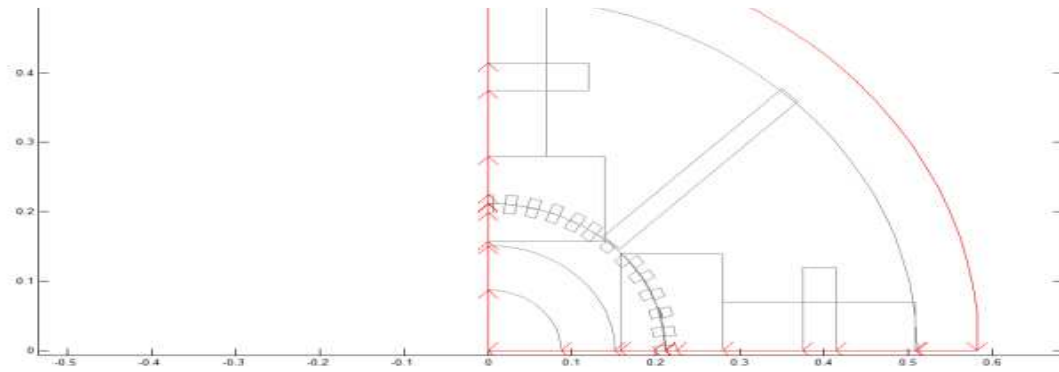


Figure 4. Stator rotor geometry of PMH stepper motor for uniform narrow air-gap (0.137 mm) with extra teeth on stator after boundary conditions implemented

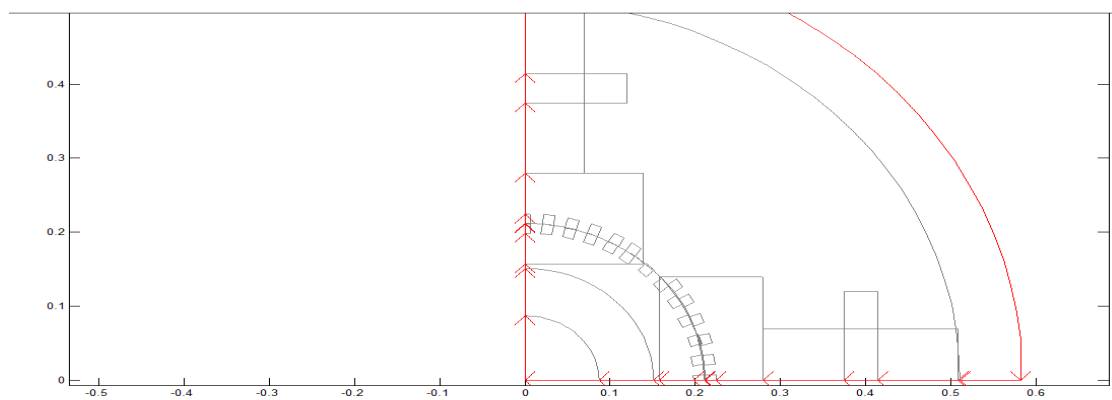


Figure 5. Stator rotor geometry of PMH stepper motor for uniform narrow air-gap (0.137 mm) without extra teeth on stator after boundary conditions implemented

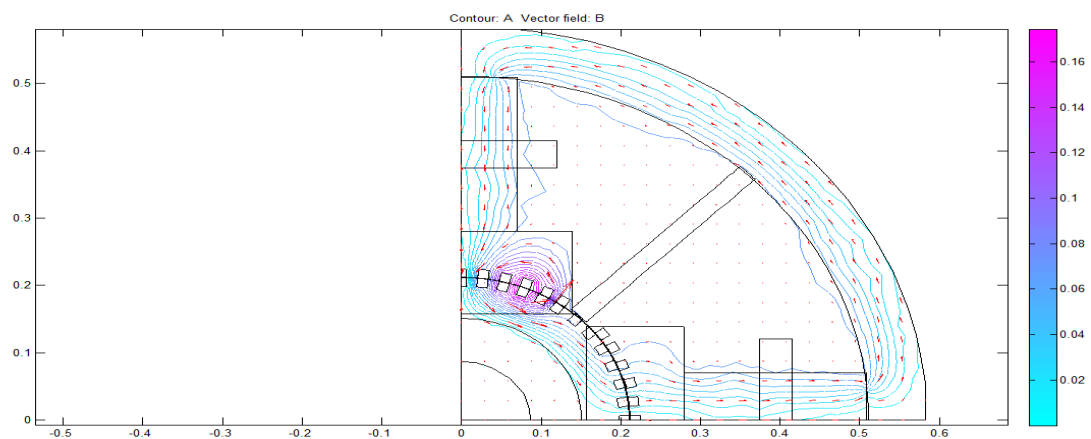


Figure 6. PDE solution for Iron (99.8%) core material with NdFeB permanent magnet with extra teeth on stator without excitation

3.3. PDE Model for Solution

In this investigation two core materials are used for investigation as iron (99.8%) and iron (99.95%). These permeability values are given for stator and rotor core material portion in the geometry shown in Figure 2 and Figure 3. Current density in these portions considered as zero.

Permanent magnet portion permeability is also calculated using (19) and current density is calculated [3]. Two types of permanent magnetic materials are used in this investigation like NdFeB, $\text{Se}_2\text{Co}_{17}$.

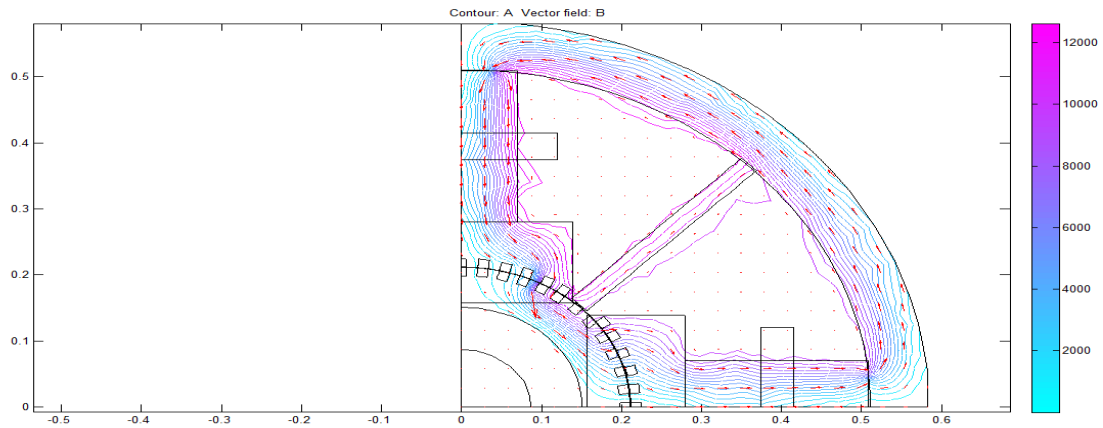


Figure 7. PDE solution for Iron (99.8%) core material with NdFeB permanent magnet with extra teeth on stator with excitation for current density of 17056A/m^2

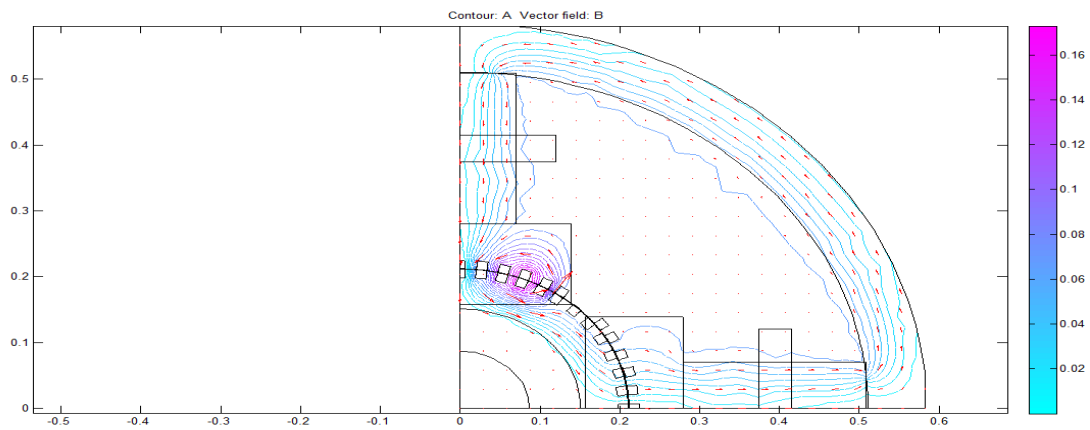


Figure 8. PDE solution for Iron (99.8%) core material with NdFeB permanent magnet without extra teeth on stator without excitation

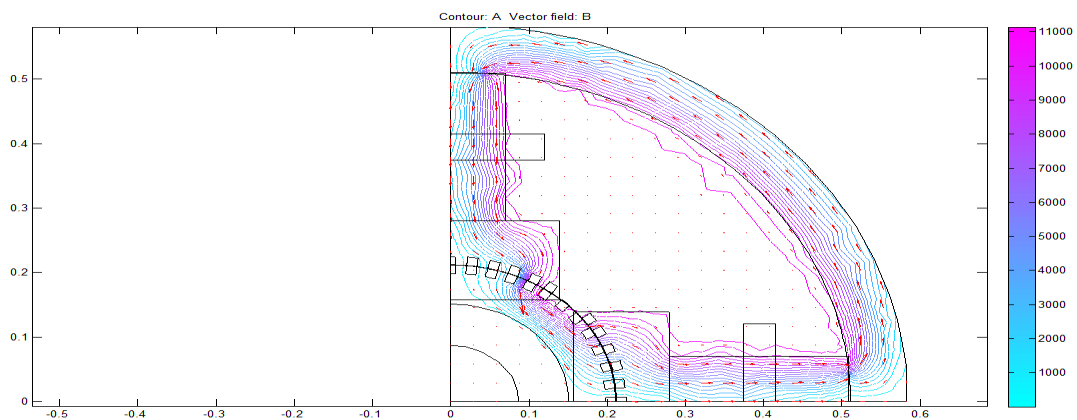


Figure 9. PDE solution for Iron (99.8%) core material with NdFeB permanent magnet with extra teeth on stator with excitation for current density of 17056A/m^2

Current density is considered zero and permeability as one for airgap and current coil to investigate permanent magnet operating point. Current density is considered for current coil to investigate total mmf under exciting condition.

Table 2. MMF due to permanent magnet and excitation coil

Topology	Stator, rotor core Iron (%)	Permanent magnet	Current density (A/m ²)	MMF due to PM, AT×10 ⁻⁴	MMF due to excitation, AT
1	Iron (99.8)	NdFeB	170648	4.578	23.6352
		Sm ₂ Co ₁₇	341296	4.578	30.7940
	Iron (99.95)	Sm ₂ Co ₁₇	170648	4.578	23.6352
		NdFeB	341296	4.578	30.7940
		Sm ₂ Co ₁₇	170648	4.578	107.779
		NdFeB	341296	4.578	230.955
2	Iron (99.8)	NdFeB	170648	4.578	30.7940
		Sm ₂ Co ₁₇	341296	4.578	38.4925
	Iron (99.95)	Sm ₂ Co ₁₇	170648	4.578	30.7940
		NdFeB	341296	4.578	38.4925
		Sm ₂ Co ₁₇	170648	6.159	92.3820
		NdFeB	341296	6.159	184.764
3	Iron (99.8)	NdFeB	170648	1.232	15.3972
		Sm ₂ Co ₁₇	341296	1.232	30.7940
	Iron (99.95)	Sm ₂ Co ₁₇	170648	1.231	15.3972
		NdFeB	341296	1.231	30.7940
		Sm ₂ Co ₁₇	170648	4.578	46.4910
		NdFeB	341296	4.578	92.3820
4	Iron (99.8)	NdFeB	170648	3.079	46.4910
		Sm ₂ Co ₁₇	341296	3.079	92.3820
	Iron (99.95)	NdFeB	170648	1.539	18.3120
		Sm ₂ Co ₁₇	341296	1.539	38.4925
		NdFeB	170648	1.539	18.3120
		Sm ₂ Co ₁₇	341296	1.539	38.4925
5	Iron (99.8)	NdFeB	170648	3.849	61.5880
		Sm ₂ Co ₁₇	341296	3.849	107.779
	Iron (99.95)	NdFeB	170648	3.849	61.5880
		Sm ₂ Co ₁₇	341296	3.849	107.779
		NdFeB	170648	0.811	4.6890
		Sm ₂ Co ₁₇	341296	0.811	9.7380
6	Iron (99.8)	NdFeB	170648	0.811	4.6890
		Sm ₂ Co ₁₇	341296	0.811	9.7380
	Iron (99.95)	NdFeB	170648	0.811	4.6890
		Sm ₂ Co ₁₇	341296	0.811	9.7380
		NdFeB	170648	0.970	9.7380
		Sm ₂ Co ₁₇	341296	0.970	16.230
7	Iron (99.8)	NdFeB	170648	0.970	9.7380
		Sm ₂ Co ₁₇	341296	0.970	16.230
	Iron (99.95)	NdFeB	170648	0.649	2.4340
		Sm ₂ Co ₁₇	341296	0.649	6.4920
		NdFeB	170648	0.649	2.4340
		Sm ₂ Co ₁₇	341296	0.649	6.4920
8	Iron (99.95)	NdFeB	170648	0.811	6.4920
		Sm ₂ Co ₁₇	341296	0.811	12.984
		NdFeB	170648	0.568	3.2460
		Sm ₂ Co ₁₇	170648	0.568	8.1150
		Sm ₂ Co ₁₇	170648	0.568	3.2460

Considering all these conditions PDE solution is obtained as shown in Figure 5, Figure 6, Figure 7, and Figure 8. Figure 5 and Figure 7 are magnetic potential diagrams for PMH stepper motor under permanent magnet excitation for with and without extra teeth on stator respectively. Figure 6 and Figure 8 are magnetic potential diagrams for PMH stepper motor under permanent magnet and current coil excitations for with and without extra teeth on stator respectively.

PDE toolbox of Matlab for FEM analysis of PMH stepper motor is used to investigate mmf due to permanent magnet for different topologies which is difficult to investigate by mathematical model. Different topologies considered are 1) Uniform air-gap (0.137 mm) with extra teeth on stator 2) Uniform air-gap (0.137 mm) without extra teeth on stator 3) Non-uniform air-gap (0.137 mm) with extra teeth on stator 4) Non-uniform air-gap (0.137 mm) without extra teeth on stator 5) Uniform air-gap (0.93 mm) with extra teeth on stator 6) Uniform air-gap (0.93 mm) without extra teeth on stator 7) Non-uniform air-gap (0.93 mm) with extra teeth on stator 8) Non-uniform air-gap (0.93 mm) without extra teeth on stator. The details of all the eight topologies are shown in Table 2.

4. Conclusion

MMF distribution of pmh stepper motor is found uniform with uniform airgap topologies (topologies 1,2 and 5,6). More mmf interaction between stator and rotor is found for low airgap topologies (0.137 mm). Leakage flux is minimized using extra teeth on stator (topologies 1,5). There is no much difference found in mmf distribution for different permanent magnetic materials (NdFeB, $\text{Sm}_2\text{Co}_{17}$). More mmf interaction observed for Iron (99.95%) core material. Time required for FEM analysis is comparatively low with FEM commercial softwares. This analysis is done without using any commercial FEM software first time for FEM analysis of Stepper motor.

References

- [1] Sutikno T. The Preliminary Research for Implementation of Improved DTC Scheme of High Performance PMSM Drives. *TELKOMNIKA Indonesian Journal of Electrical Engineering*. 2008; 6(3): 155-166.
- [2] H. Chai. A Mathematical Model for Single-Stack Step Motors. *IEEE Transactions on Power Apparatus and Systems*. 1975; 94(5).
- [3] KR Rajagopal, M. Krishnaswamy, Bhim Singh and B. P. Singh. An Improved High-Resolution Hybrid Stepper Motor for Solar-Array Drive of Indian Remote-Sensing Satellite. *IEEE Transactions on Industry Applications*. 1997; 33(4).
- [4] KR Rajagopal, Bhim Singh and B. P. Singh. Effects of Non-Uniform Airgap and Hysteresis on the Performance of Hybrid Stepper Motor. *IEEE transactions on Industry Applications*. 1998; 34(3).
- [5] Dou Yiping. *The Engineering Rationality of a Hybrid Stepping Motor Calculation Model*. Proceedings of the CSEE. 1999; 19(5): 35-38.
- [6] Praveen RP, Ravichandran MH, VT Sadasivan Achari, Jagathy Raj VP, G Madhu and R Bindu. Design and Finite Element Analysis of Hybrid Stepper Motor for Spacecraft Applications', *IEEE transactions on Magnetics*. 2009; 45(4).
- [7] Khairudin M. Dynamic Modelling of a Flexible Link Manipulator Robot Using AMM. *TELKOMNIKA Indonesian Journal of Electrical Engineering*. 2008; 6(3): 185-190.
- [8] Juha Pyrhönen, Tapani Jokinen, Val'eria Hrabovcov'a. Design of Rotating Electrical Machines. John Wiley & Sons, Ltd. 2008.
- [9] Jacek F. Gieras, Mitchell Wing. Permanent Magnet Motor Technology Design and Applications. Marcel Dckker Inc. New York, USA.
- [10] Golub, Gene H., and Charles F. Van Loan, Matrix Computations. 2nd edition. Johns Hopkins University Press, Baltimore. MD. 1989.
- [11] Yousef Saad. Variations on Arnoldi's Method for Computing Eigenvalues of Large Unsymmetric Matrices. *Linear Algebra and its Applications*. 1980; 34: 269-295.